

# An improved 2D time-to-collision for articulated vehicles: predicting sideswipe and rear-end collisions

Abhijeet Behera<sup>a,b,\*</sup>, Sogol Kharrazi<sup>a,b</sup>, Erik Frisk<sup>b</sup> and Maytheewat Aramrattana<sup>a</sup>

<sup>a</sup> The Swedish National Road and Transport Research Institute, Linköping, 58330, Sweden

<sup>b</sup> Division of Vehicular Systems, Electrical Engineering, Linköping University, Sweden

## ARTICLE INFO

### Keywords:

Time-to-collision

TTC

Two-dimensional time-to-collision

TTC<sub>2D</sub>

Articulated vehicles

Tractor-semitrailer

Rear-end collision

Sideswipe collision

CARLA

## ABSTRACT

Time-to-collision (TTC) is a widely used measure for estimating the time until a rear-end collision between two vehicles, assuming both maintain constant speeds and headings in the prediction horizon. To also capture sideswipe collisions, a two-dimensional extension, TTC<sub>2D</sub>, was introduced. However, this formulation assumes both vehicles have the same heading and that their headings remain unchanged during the manoeuvre, in addition to the standard assumptions on the prediction horizon. Moreover, its use for articulated vehicles like a tractor-semitrailer remains unclear. This paper addresses these limitations by developing three enhanced versions of TTC<sub>2D</sub>. The first incorporates vehicle heading information, which is missing in the original formulation. The standard assumption of constant speed and heading in the prediction horizon holds. The second adapts this to articulated vehicles while retaining the assumptions of the first version. The third version maintains the constant heading assumption but relaxes the constant speed assumption by allowing constant acceleration. The versions are tested in a cut-in scenario using the CARLA simulation environment. They detect rear-end collisions, similar to TTC, and moreover, they also identify sideswipe risks, something TTC could not predict.

## 1. Introduction

Safety is a cornerstone of transportation planning and traffic management, impacting public health, infrastructure design, and economic efficiency. Traditional safety evaluation methods often rely on historical crash data to assess and mitigate risks (Abdel-Aty and Pande, 2007). While these approaches provide valuable insights, they are inherently reactive, requiring accidents to occur before actionable conclusions can be drawn. This dependency on past incidents poses significant challenges, including ethical concerns, data limitations, and delays in addressing emerging safety issues (Tarko, 2018). In this context, surrogate safety measures (SSMs) have emerged as a proactive and effective alternative for assessing traffic safety. It is a proxy that quantifies safety risks by measuring the likelihood of potential crashes. These measures rely on near-miss events, conflict analyses, and observable indicators, such as vehicle trajectories and traffic interactions, to predict and prevent accidents before they occur.

The inception of SSMs can be traced back to the early 1970s (Hayward, 1971), and considerable research has been done around it since then. Over the years, numerous SSMs have been developed to address a wide range of safety challenges. Researchers have adopted various approaches to categorise these SSMs. Wang, Xie, Huang and Liu (2021) and Mahmud, Ferreira, Hoque and Tavassoli (2017) provide a comprehensive review of SSMs and their categorisation. More specific analyses focusing on intersections and vulnerable road users are presented by Sarkar, Rao and Chatterjee (2024) and Johnsson, Lareshyn and De Ceunynck (2018), respectively. Based on these studies, SSMs can be generally classified into four broad categories: Time, Distance, Deceleration, and Energy. Time-based SSMs include measures such as time-to-collision (TTC) and other variants of TTC developed over the years, post-encroachment time, time-to-accident, gap, headway, etc. Distance-based SSMs comprise measures such as proportional stopping distance, unsafe density, etc. Deceleration-based SSMs encompass measures such as deceleration rate to avoid collision, crash potential index, etc. Energy-based SSMs involve measures such as crash severity, crash index, deltaV, etc. The previously referenced review articles discuss detailed definitions and studies associated with each measure.

Time-to-Collision (TTC) is one of the most widely utilised surrogate safety measures (SSMs) in collision avoidance systems. It is primarily designed to predict rear-end collisions, where one vehicle impacts the rear of another (Hayward,

\*Corresponding author

 abhijeet.behera@vti.se (A. Behera)

ORCID(s): 0009-0000-0356-7799 (A. Behera)

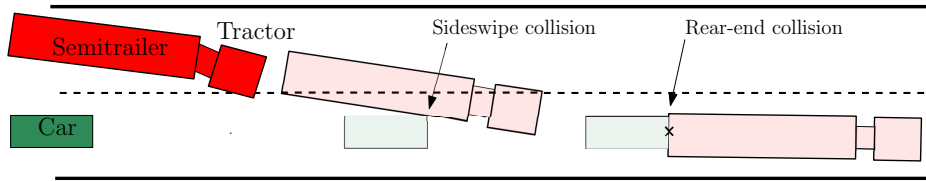


**Figure 1:** Collision between a tractor-semitrailer and a car during a lane change initiated by tractor-semitrailer.

1972). However, the conventional formulation of TTC does not account for the risk of lateral collisions, such as sideswipes, where contact occurs along the sides of the vehicles. For relatively short vehicles, such as passenger cars, the distinction between longitudinal and lateral collisions is less critical, since their dimensions in both directions are relatively similar. In such cases, even if a lateral collision occurs but a longitudinal collision is predicted, the discrepancy in collision timing is typically small. However, this assumption does not hold for long articulated vehicles, such as tractor-semitrailers. Due to their significantly greater length compared to width, the physical dimensions introduce a larger disparity between longitudinal and lateral collision risks. As a result, predicting collisions in only one direction (typically longitudinal) may overlook critical side-impact scenarios. Figure 1 illustrates two potential collision types that can arise when a tractor-semitrailer cuts into the path of a car. It may be argued that preventing a rear-end collision would inherently eliminate the risk of a sideswipe collision in scenarios shown in Figure 1. For instance, if a rear-end collision is anticipated, the tractor-semitrailer could avoid initiating the cut-in manoeuvre, thereby preventing both collisions. However, this approach results in an overly cautious driving style, which can lead to traffic flow disruptions (Haué and Merlhiot, 2024).

Several variants of TTC have been proposed, including time-exposed TTC, time-integrated TTC, and modified TTC (Minderhoud and Bovy, 2001; Ozbay, Yang, Bartin and Mudigonda, 2008). However, these formulations retain the core assumptions of the conventional TTC and are limited to longitudinal motion. To overcome this, Hou, List and Guo (2014) introduced a geometric approach that considers both longitudinal and lateral directions by solving two-dimensional distance equations, while Ward, Agamennoni, Worrall, Bender and Nebot (2015) proposed a looming-based method to evaluate collision risk in two dimensions. Building on these efforts, Guo, Xie and Keyvan-Ekbatani (2023) proposed a two-dimensional TTC ( $TTC_{2D}$ ) that relaxes several simplifying assumptions of conventional TTC and quantifies collision risk in both longitudinal and lateral directions. The formulation assumes that both vehicles maintain identical and constant headings throughout the manoeuvre. While this assumption may be reasonable for gradual manoeuvres, such as long-distance highway lane changes, it becomes inadequate in scenarios involving substantial changes in heading angle, including short-distance lane changes, intersections, and roundabouts. These limitations become more pronounced in the case of articulated vehicles, such as a tractor and semitrailer, where the tractor and trailer may each have different heading angles relative to the same vehicle. It is unclear how to apply this measure to a tractor-semitrailer. This paper addresses these limitations by proposing an enhanced version of  $TTC_{2D}$  that incorporates vehicle orientation and demonstrates its applicability to a tractor-semitrailer combination.

To evaluate newly developed surrogate safety measures (SSMs), researchers typically adopt one of two primary approaches: analysis of historical crash data (e.g., Nikolaou, Ziakopoulos and Yannis (2023); Xie, Yang, Ozbay and Yang (2019)) or simulation-based evaluation (e.g., Morando, Tian, Truong and Vu (2018); So, Dedes, Park, HosseinyAlamdary and Grejner-Brzezinsk (2015)). The traditional data-driven approach assesses the correlation between SSM outputs and observed crash frequencies or severities. While this method provides valuable empirical insights, it is often constrained by the availability and quality of crash data, and the time required to collect sufficient data, particularly for rare crash types (He, Qin, Liu and Sayed, 2018). As a result, simulation-based methods are gaining popularity, especially those leveraging high-fidelity platforms such as CARLA (Dosovitskiy, Ros, Codevilla, Lopez and Koltun, 2017). Consequently, this paper employs the CARLA to evaluate the proposed enhanced  $TTC_{2D}$  measure.

Therefore, the main contributions of this paper are summarised as follows:

- Development of a more generalised version of  $TTC_{2D}$  that considers the orientation of the vehicles and extends its applicability to a tractor-semitrailer.
- An investigation into how the improved  $TTC_{2D}$  compares to conventional TTC and existing  $TTC_{2D}$  in a synthetic scenario (similar to that shown in Figure 3) simulated in CARLA.

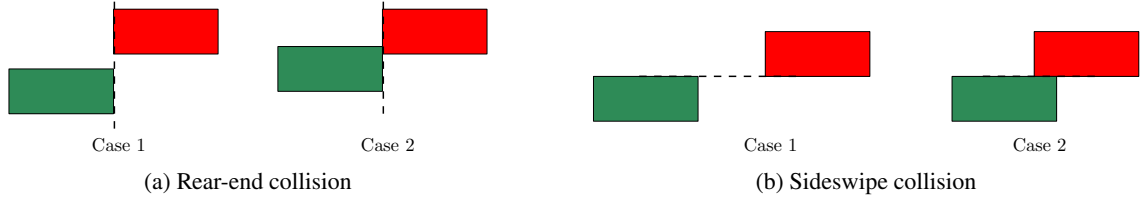


**Figure 2:** Prospective collision scenarios. Red and green denote the lead and following cars, respectively.

## 2. Description of existing two-dimensional TTC

Conventional Time-to-Collision (TTC) is defined exclusively for longitudinal motion and represents the time required for a collision to occur between two vehicles, under the assumption that both maintain their current speeds and headings. The mathematical expression for TTC is given by,

$$\text{TTC} = \begin{cases} \frac{s_{0\text{lon}} - l}{v_{\text{lon}} - v_{0\text{lon}}}, & v_{\text{lon}} > v_{0\text{lon}}, \\ \infty, & \text{otherwise.} \end{cases} \quad (1)$$

$s_{0\text{lon}}$  is the longitudinal distance between the front ends of two vehicles,  $v_{0\text{lon}}$  and  $v_{\text{lon}}$  are the longitudinal speed of the leading and following vehicles, respectively, and  $l$  is the length of the leading vehicle.

Guo et al. (2023) extended the conventional definition of TTC by incorporating both longitudinal and lateral components. The resulting expression to compute  $\text{TTC}_{2\text{D}}$  is given by,

$$\text{TTC}_{\text{lon}} = \begin{cases} \frac{s_{0\text{lon}} - l}{v_{\text{lon}} - v_{0\text{lon}}} : & s_{0\text{lon}} > l \quad \& \quad v_{\text{lon}} > v_{0\text{lon}} \quad \& \quad s_{0\text{lat}} - (v_{\text{lat}} - v_{0\text{lat}}) \frac{s_{0\text{lon}} - l}{v_{\text{lon}} - v_{0\text{lon}}} < w, \\ \infty : & \text{otherwise.} \end{cases} \quad (2a)$$

$$\text{TTC}_{\text{lat}} = \begin{cases} \frac{s_{0\text{lat}} - w}{v_{\text{lat}} - v_{0\text{lat}}} : & s_{0\text{lat}} > w \quad \& \quad v_{\text{lat}} > v_{0\text{lat}} \quad \& \quad s_{0\text{lon}} - (v_{\text{lon}} - v_{0\text{lon}}) \frac{s_{0\text{lat}} - w}{v_{\text{lat}} - v_{0\text{lat}}} < l, \\ \infty : & \text{otherwise.} \end{cases} \quad (2b)$$

$$\text{TTC}_{2\text{D}} = \min(\text{TTC}_{\text{lon}}, \text{TTC}_{\text{lat}}). \quad (2c)$$

where  $\text{TTC}_{\text{lon}}$  is the time-to-collision in the longitudinal direction, and  $\text{TTC}_{\text{lat}}$  is the time-to-collision in the lateral direction.  $s_{0\text{lat}}$  is the initial lateral distance between the central longitudinal axes of the two vehicles,  $v_{0\text{lat}}$  and  $v_{\text{lat}}$  are the lateral speed of the leading and following vehicles, respectively, and  $w$  is the width of the vehicle.

The first case outlined in (2a) and (2b) are based on three conditions: a) There is no collision between the vehicles at the current time, b) vehicles approach each other at a positive rate, c) there is a lateral overlap at the predicted time of longitudinal collision,  $\text{TTC}_{\text{lon}}$  and a longitudinal overlap at the time of lateral collision,  $\text{TTC}_{\text{lat}}$ . At the predicted time of collision in each direction, two possible scenarios can arise, as illustrated in Figure 2. In Case 1, there is either longitudinal or lateral overlap, but not both. Hence, a collision does not occur. A collision occurs only in Case 2, where both longitudinal and lateral overlaps are present. The third condition in the first case of equations (2a) and (2b) ensures that Case 2 is obtained.

It is evident from (2) that the coordinate systems of the lead and following vehicles are assumed to be aligned with each other. However, this assumption does not generally hold in real-world scenarios, where the orientations of the two vehicles may differ significantly. This misalignment affects both the computed distance between the vehicles and the relative speed with which they approach one another. The problem becomes challenging with an articulated vehicle, as different units of the articulated vehicle will have different orientations. In the next section, a generalised  $\text{TTC}_{2\text{D}}$  is developed to address the aforementioned limitations.

### 3. Mathematical Formulation

The development of more generalised  $TTC_{2D}$  is carried out through a sequence of improvements to the baseline formulation in (2). First in Section 3.1, the formulation is extended to account for vehicle orientation, assuming non-articulated vehicles. The formulation is then refined in Section 3.2 to accommodate articulated vehicle configurations, such as tractor–semitrailer combinations. Subsequently, the formulation is further developed in Section 3.3 to relax the assumption of constant speed in the prediction horizon. It may be noted that in the first two sections, similar to the existing formulation of  $TTC_{2D}$  and the conventional TTC, constant speed and orientation (or heading) are assumed in the prediction horizon.

#### 3.1. Collision between two vehicles (no articulation)

Figure 3 illustrates the coordinate system employed for calculating the relative position and velocity of the vehicles involved. Local coordinate frames, defined in accordance with the ISO vehicle frame, are fixed to the following (green) vehicle at point  $R$  and to the lead (red) vehicle at point  $A$ , both located at the midpoints of the front edges of the respective vehicles. All computations are performed with respect to the coordinate frame of the following vehicle ( $R$ ), such that the position and velocity of the lead vehicle are expressed in the  $R$ -based coordinate system. This frame comprises a longitudinal axis ( $X$ ) and a lateral axis ( $Y$ ). The quantities  $s_{0X}$  and  $s_{0Y}$  denote the relative position of point  $A$  with respect to point  $R$  along the  $X$  and  $Y$  axes, respectively.

In this formulation, the (lon, lat) representation used in the baseline model (see 2) is replaced by the ( $X$ ,  $Y$ ) coordinate system. Let  $(l_1, w_1, \psi_1)$  represent the length, width, and yaw angle of the lead vehicle, and  $(l, w, \psi)$  refer to the following vehicle. To account for vehicle orientations, two changes are made to the baseline formulation in (2): a) the effective projections of the lead vehicle's length and width onto the  $X$  and  $Y$  axes, denoted as  $c_{0X}$  and  $c_{0Y}$  respectively, are used in place of  $l$  and  $w$  in the baseline, b) the longitudinal and lateral speeds of the lead vehicle, represented as  $v_{0x}$  and  $v_{0y}$  in  $x - y$  coordinate system, are transformed in the  $R$ -based coordinate system, denoted as  $v_{0X}$  and  $v_{0Y}$ . The projections are computed as follows,

$$\begin{bmatrix} c_{0X} \\ c_{0Y} \end{bmatrix} = R_0 \begin{bmatrix} l_0 \\ \frac{w_0}{2} \end{bmatrix} \quad (3)$$

where  $R_0$  is the rotation matrix given by,

$$R_0 = \begin{bmatrix} \cos(\psi_0 - \psi) & -\sin(\psi_0 - \psi) \\ \sin(\psi_0 - \psi) & \cos(\psi_0 - \psi) \end{bmatrix}. \quad (4)$$

Using the defined rotation matrix, the longitudinal and lateral speeds of the lead vehicle in the coordinate system of the following vehicle are obtained as,

$$\begin{bmatrix} v_{0X} \\ v_{0Y} \end{bmatrix} = R_0 \begin{bmatrix} v_{0x} \\ v_{0y} \end{bmatrix} \quad (5)$$

where  $v_{0x}$  and  $v_{0y}$  are the longitudinal and lateral speeds of the lead vehicle in its local coordinate system ( $x, y$ ).

The resulting expression to compute  $TTC_{2D}^1$  (superscript 1 indicates first version) is given by,

$$TTC_{0X} = \begin{cases} \frac{s_{0X} - c_{0X}}{v_X - v_{0X}} : & s_{0X} > c_{0X} \quad \& \quad v_X > v_{0X} \quad \& \quad s_{0X} - (v_Y - v_{0Y}) \frac{s_{0X} - c_{0X}}{v_X - v_{0X}} < c_{0Y}, \\ \infty : & \text{otherwise.} \end{cases} \quad (6a)$$

$$TTC_{0Y} = \begin{cases} \frac{s_{0Y} - c_{0Y} - \frac{w}{2}}{v_Y - v_{0Y}} : & s_{0Y} > c_{0Y} + \frac{w}{2} \quad \& \quad v_Y > v_{0Y} \quad \& \quad s_{0X} - (v_X - v_{0X}) \frac{s_{0Y} - c_{0Y} - \frac{w}{2}}{v_Y - v_{0Y}} < c_{0X}, \\ \infty : & \text{otherwise.} \end{cases} \quad (6b)$$

$$TTC_{2D}^1 = \min(TTC_{0X}, TTC_{0Y}). \quad (6c)$$

Note that these expressions are similar to (2), but they take into account the projected lengths and widths, as well as the lead vehicle's longitudinal and lateral speeds, transformed into the coordinate frame of the following vehicle.

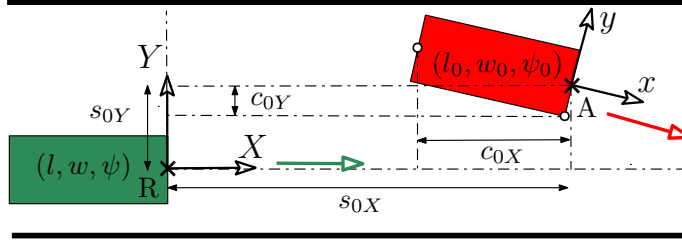


Figure 3: Schematic of scenario and employed coordinate system.

### 3.2. Collision between a tractor-semitrailer and a car

Figure 4 shows the coordinate system employed for calculating the relative position of the tractor-semitrailer (red) with respect to the car (green). The specifics of the coordinate system and the vehicle dimensions are analogous to the first version. The difference lies in the type of vehicles considered in this version. The tractor-semitrailer is an articulated vehicle, and hence, the articulation constraint is incorporated into the computation process. First, the measure  $TTC_{2D,0}$  is computed for the collision between the tractor and the car. Since neither of them is an articulated vehicle, the computation process is similar to the first version. After determining the  $TTC_{2D,0}$  between the tractor and the car, a check is conducted to assess whether the semitrailer will collide with the car, given the tractor's trajectory. The measure  $TTC_{2D,1}$  is computed between the semitrailer and the car. Subsequently,  $TTC_{2D}^2$  is determined as the minimum of the measures derived from individual units. This approach accounts for the physical coupling between the tractor and semitrailer, ensuring that the semitrailer's collision risk is evaluated based on the tractor's trajectory and articulation angle.

#### 3.2.1. TTC between the tractor and car

The computation of  $TTC_{2D,0}$  between the tractor and the car follows the same procedure as the first version. Accordingly, the expressions derived in (6) remain applicable in this version.

#### 3.2.2. TTC between the semitrailer and car

A collision with the semitrailer can occur before a collision with the tractor. Given the trajectory of the tractor with respect to the car, the task is to identify the corresponding trajectory of the semitrailer with respect to the car. The forward euler discretisation method is employed to iteratively calculate the relative position of the tractor with respect to the car at each time step ( $\Delta t$ ) until a collision occurs at time  $TTC_{2D,0}$ . The corresponding expressions read as,

$$\begin{aligned} s_{0X}(t) &= s_{0X}(t-1) + (v_X - v_{0X}) \Delta t, \\ s_{0Y}(t) &= s_{0Y}(t-1) + (v_Y - v_{0Y}) \Delta t, \end{aligned} \quad (7)$$

where the longitudinal ( $v_{0X}$ ) and lateral ( $v_{0Y}$ ) speeds are calculated in (5). The heading of the tractor ( $\psi_0$ ) stays constant for the entire computation duration of  $TTC_{2D,0}$ , the time of first contact between the tractor and the car. An analytical expression for the heading of the semitrailer ( $\psi_1$ ) is derived in Appendix A, see (28). Using the expressions for heading angles, the semitrailer's relative position with respect to the car ( $s_{1X}, s_{1Y}$ ) at each time step is given by,

$$\begin{aligned} s_{1X}(t) &= s_{0X}(t) - l_{fa} \cos(\psi_0(t) - \psi(t)) + l_{ra} \cos(\psi_1(t) - \psi(t)), \\ s_{1Y}(t) &= s_{0Y}(t) - l_{fa} \sin(\psi_0(t) - \psi(t)) + l_{ra} \sin(\psi_1(t) - \psi(t)), \end{aligned} \quad (8)$$

where  $l_{fa}$  is the distance of the tractor's front edge, *A* in Figure 4, from the articulation joint *C*.  $l_{ra}$  is the distance of the semitrailer's front edge, *B* in Figure 4, from the articulation joint *C*. Let the projection of the semitrailer's length and width onto the *X* and *Y* axes be denoted as  $c_{1X}$  and  $c_{1Y}$ . They are given by,

$$\begin{bmatrix} c_{1X} \\ c_{1Y} \end{bmatrix} = R_1 \begin{bmatrix} l_1 \\ w_1 \\ 2 \end{bmatrix} \quad (9)$$

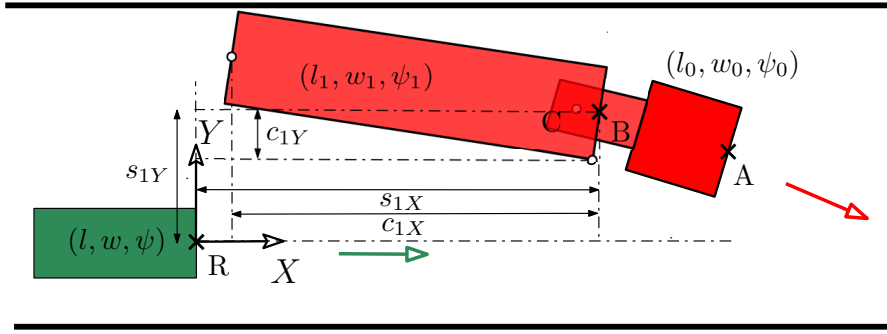


**Figure 4:** Schematic of scenario and employed coordinate system for the semitrailer of the articulated vehicle. The coordinate system for the tractor is the same as Figure 3.

where  $R_1$  is the rotation matrix given by,

$$R_1 = \begin{bmatrix} \cos(\psi_1 - \psi) & -\sin(\psi_1 - \psi) \\ \sin(\psi_1 - \psi) & \cos(\psi_1 - \psi) \end{bmatrix}. \quad (10)$$

The time-to-collision between the semitrailer and the car, denoted as  $TTC_{2D,1}$ , accounting for both longitudinal and lateral interactions, is defined as,

$$TTC_{1X} = \begin{cases} t^* : & s_{1X}(t_0) > c_{1X}(t_0) \quad \& \quad s_{1Y}(t^*) < c_{1Y}(t^*) + \frac{w}{2} \quad \& \quad s_{1X}(t^*) - c_{1X}(t^*) < \epsilon_X, \\ \infty : & \text{otherwise.} \end{cases} \quad (11a)$$

$$TTC_{1Y} = \begin{cases} t^* : & s_{1Y}(t_0) > c_{1Y}(t_0) + \frac{w}{2} \quad \& \quad s_{1X}(t^*) < c_{1X}(t^*) \quad \& \quad s_{1Y}(t^*) - c_{1Y}(t^*) - \frac{w}{2} < \epsilon_Y, \\ \infty : & \text{otherwise.} \end{cases} \quad (11b)$$

$$TTC_{2D,1} = \min(TTC_{1X}, TTC_{1Y}). \quad (11c)$$

where  $t = t^*$  indicates the time stamp of the first contact (longitudinal or lateral) between the semitrailer and the car,  $(\epsilon_X, \epsilon_Y) > 0$  are small positive constants selected to account for numerical approximations in longitudinal and lateral contacts, respectively. The longitudinal and lateral collisions between the semitrailer and the car are checked at every time step in the prediction horizon using (11a) and (11b) respectively. Similar to (2), there are three conditions for the first case in each of these expressions. The first condition ensures that there is no collision between the semitrailer and the car at the initial time  $t = t_0$ . The second and third conditions are satisfied only when there is a lateral overlap at the predicted time of longitudinal contact or a longitudinal overlap at the time of lateral contact, respectively.

Finally, the overall two-dimensional time-to-collision for the combined tractor-semitrailer system, denoted by  $TTC_{2D}^2$  (superscript 2 indicates second version) is computed as,

$$TTC_{2D}^2 = \min(TTC_{2D,0}, TTC_{2D,1}). \quad (12)$$

### 3.3. Collision between a tractor-semitrailer and a car assuming constant acceleration and heading in the prediction horizon

In this version, the assumption of constant speed in the prediction horizon is replaced with constant acceleration for both vehicles, while retaining the constant heading assumption. This modified version of  $TTC_{2D}$ , denoted as  $TTC_{2D}^3$ , is similar to modified TTC, a variant of conventional TTC (Ozby et al., 2008). The difference is that modified TTC operates in one dimension, whereas  $TTC_{2D}^3$  works in two dimensions.

The calculation procedure follows the same approach as in the previous version, but now incorporates accelerations in both the longitudinal and lateral directions for the tractor-semitrailer and the car. As a result, some of the expressions derived in the second version are reformulated to include acceleration-based terms. In practice, it is not straightforward for the tractor-semitrailer to obtain the acceleration of the car. However, it is expected that with new technologies, it will become easy to estimate it.

### 3.3.1. TTC between the tractor and car

Let  $(a_X, a_Y)$  denote the longitudinal and lateral acceleration of the car in its local coordinate system  $(X, Y)$ . The accelerations of the tractor, transformed into the car's coordinate frame, are denoted by  $(a_{0X}, a_{0Y})$ , and are computed as follows.

$$\begin{bmatrix} a_{0X} \\ a_{0Y} \end{bmatrix} = R_0 \begin{bmatrix} a_{0x} - v_{0y}\dot{\psi}_0 \\ a_{0y} + v_{0x}\dot{\psi}_0 \end{bmatrix}, \quad (13)$$

where  $a_{0x}$  and  $a_{0y}$  are the longitudinal and lateral speeds of the tractor in its local coordinate system  $(x, y)$  and  $\dot{\psi}_0$  is the yaw rate of the tractor. Note that the heading of the tractor can change in real-time, but is constant in the prediction horizon. The same holds for the car. Since the car is travelling straight and the cut-in executed by the tractor-semitrailer, the yaw rate of the car and the corresponding Coriolis forces are assumed to be negligible.

Given the relative position, speed, and acceleration, the expressions that govern the tractor's and car's motion in both longitudinal and lateral directions are formulated. These are quadratic equations in time, whose roots determine the time required for the car to collide with the tractor, assuming both vehicles maintain their current headings. The quadratic equations read as,

$$\begin{aligned} s_{0X} &= (v_X - v_{0X}) t_{0X} + 0.5 (a_X - a_{0X}) t_{0X}^2, \\ s_{0Y} &= (v_Y - v_{0Y}) t_{0Y} + 0.5 (a_Y - a_{0Y}) t_{0Y}^2. \end{aligned} \quad (14)$$

Each of the quadratic equations has two roots given by,

$$\begin{aligned} t_{0X} &= \frac{-(v_X - v_{0X}) \pm \sqrt{(v_X - v_{0X})^2 + 2 (a_X - a_{0X}) s_{0X}}}{a_X - a_{0X}}, \quad \text{for } a_X \neq a_{0X}, \\ t_{0Y} &= \frac{-(v_Y - v_{0Y}) \pm \sqrt{(v_Y - v_{0Y})^2 + 2 (a_Y - a_{0Y}) s_{0Y}}}{a_Y - a_{0Y}}, \quad \text{for } a_Y \neq a_{0Y}. \end{aligned} \quad (15)$$

Since roots are representative of the time required for the collision, the smallest positive real root out of the two from each of the above expressions is selected. The selected roots, denoted as  $t_{0X}^*$  for longitudinal and  $t_{0Y}^*$  for lateral, are used to determine the final relative position. Consequently, the time-to-collision between the tractor and the car ( $TTC_{2D,1}$ ) are determined as follows,

$$TTC_{0X} = \begin{cases} t_{0X}^* & : \quad s_{0X} > c_{0X} \quad \& \quad s_{0Y} - (v_Y - v_{0Y}) t_{0X}^* + 0.5 (a_Y - a_{0Y}) t_{0X}^{*2} < c_{0Y} + \frac{w}{2}, \\ \infty & : \quad \text{otherwise.} \end{cases} \quad (16a)$$

$$TTC_{0Y} = \begin{cases} t_{0Y}^* & : \quad s_{0Y} > c_{0Y} + \frac{w}{2} \quad \& \quad s_{0X} - (v_X - v_{0X}) t_{0Y}^* + 0.5 (a_X - a_{0X}) t_{0Y}^{*2} < c_{0X}, \\ \infty & : \quad \text{otherwise.} \end{cases} \quad (16b)$$

$$TTC_{2D,0} = \min (TTC_{0X}, TTC_{0Y}). \quad (16c)$$

In contrast to (6), there are two conditions for the first case in (16a) and (16b). Since the vehicles are no longer moving at constant speed, the speed constraints do not hold and are replaced by new constraints obtained using (14) and (15). The first condition checks that there is no collision between the vehicles at the current time. In the second condition, the final relative position is computed by considering constant acceleration instead of constant speed.

### 3.3.2. TTC between the semitrailer and car

There are only two changes compared to the second version. The rest of the expressions stay the same. First, the expressions in (7) are reformulated to include the acceleration terms. The modified expressions read as,

$$\begin{aligned} s_{0X}(t) &= s_{0X}(t-1) + (v_X - v_{0X}) \Delta t + 0.5 (a_X - a_{0X}) (\Delta t)^2, \\ s_{0Y}(t) &= s_{0Y}(t-1) + (v_Y - v_{0Y}) \Delta t + 0.5 (a_Y - a_{0Y}) (\Delta t)^2. \end{aligned} \quad (17)$$



(a) Tractor-semitrailer.



(b) Sideswipe collision.

**Figure 5:** Scenario in CARLA.

The second modification involves using the expression derived in (30) in Appendix A for the semitrailer's heading angle, instead of (28). Note that the new heading angle expression is derived after relaxing the assumption of constant speed. This updated expression is incorporated into the expressions presented in (8) and (9).

The final set of expressions for calculating the time to collision between the semitrailer and the car  $TTC_{2D,1}$  are the same as (11). Consequently, the measure  $TTC_{2D}^3$  (superscript 3 indicates third version) is determined as,

$$TTC_{2D}^3 = \min(TTC_{2D,0}, TTC_{2D,1}). \quad (18)$$

The versions are formulated for scenarios where the car approaches the tractor-semitrailer from behind. However, they can be easily adapted for cases where the tractor-semitrailer approaches the car from behind. This adaptation requires replacing the tractor or semitrailer length with the car's length in all relevant expressions. Additionally, the relative longitudinal speed of the car with respect to the tractor-semitrailer must be negative to ensure a positive approach rate of the tractor-semitrailer towards the car.

#### 4. Scenario description in CARLA

The developed versions are evaluated using a cut-in scenario created in the CARLA simulation environment. This scenario involves two actors: a car and a tractor-semitrailer. While the car model is available in the CARLA vehicle library, it is not the same for the tractor-semitrailer. Building on the work of Attard and Bajada (2024), a realistic model of a tractor-semitrailer is developed in the CARLA (Behera, Kharrazi and Frisk, 2025). This model is used for the analysis in this study.

Figure 5a presents the graphics of the tractor-semitrailer vehicle within the CARLA environment. The underlying physics model has been improved to address the limitations posed by the previous model developed by Attard and Bajada (2024). Furthermore, the model is also validated using the real-world measurements in Behera et al. (2025), ensuring greater fidelity to real-world vehicle dynamics.

The objective of the evaluation process is to detect sideswipe collision, shown in Figure 5b, using the developed versions of  $TTC_{2D}$ . Hence, the trajectories (speed and steering angles) of the vehicles in the scenario are specifically designed to result in a sideswipe collision. The conventional TTC operates in one dimension and does not predict such collisions because it does not account for the vehicle width. Figure 6 shows the path followed by the vehicles. The labels in the figure indicate their relative position.  $A$  is the starting location for both vehicles. When the tractor-semitrailer is at  $B$ , the car starts from rest at  $A$ . The tractor-semitrailer initiates the cut-in at  $D$ . During this time, the car is at  $C$ . Finally, both vehicles collide at  $E$ . The corresponding vehicle inputs and the variation of the distance between them are presented in Figure 7.

Figure 7a presents the speed and time profiles at different locations for both the tractor-semitrailer and the car, along with the tire steering angle. The figure indicates that the car begins its motion approximately 10 s after the tractor-semitrailer. However, due to the car's significantly greater acceleration, the distance between the two vehicles decreases rapidly. Figure 7b shows the longitudinal and lateral distance variations between the vehicles. The longitudinal distance, measured between rear edges, is negative when the tractor or semitrailer trails behind the car (e.g., at points  $A$  and  $E$ ). The longitudinal gap increases until point  $B$  as the car is stationary, then decreases due to its acceleration when the car starts moving. The lateral distance denotes the minimum gap between side edges. It remains nearly constant



**Figure 6:** Schematic of cut-in scenario executed in CARLA. Red: Tractor, Blue: Semitrailer and Green: Car.

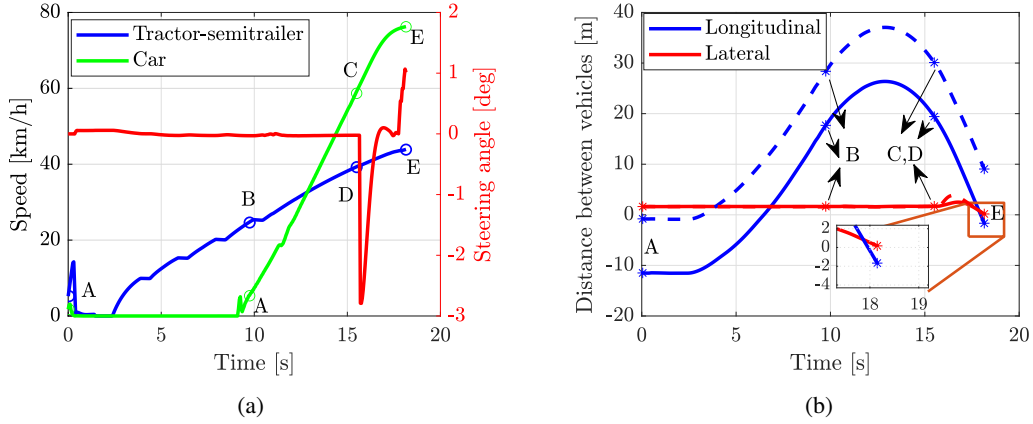


**Figure 7:** (a) Vehicle inputs in the cut-in scenario: speed of the tractor-semitrailer and the car, steering angle at the tire for the tractor, (b) Variation of distance between the tractor and the car (dashed) and the semitrailer and the car (solid) in the scenario.

until point *D*, as both vehicles initially travel in separate lanes (see Figure 6). At *D*, the tractor-semitrailer begins a cut-in. By point *E*, the semitrailer is beside the car, and a lateral distance of zero results in a sideswipe collision.

## 5. Discussions

In this section, the scenario described previously is used to evaluate the performance of the developed measures, with particular focus on Versions 2 and 3. Version 1 is excluded from the analysis, as it is designed for non-articulated vehicles, whereas this study focuses on articulated configurations. Nonetheless, Version 2, which is tailored for tractor-semitrailers, can be viewed as a natural extension of Version 1. The validity of Version 2 implicitly supports the effectiveness of Version 1 for non-articulated vehicles. The TTC value is set to  $\infty$  when no collision occurs. According to Tidwell, Blanco, Trimble, Atwood and Morgan (2015), the perception response time of a heavy vehicle driver to a collision warning is typically about 1 to 1.5 seconds under normal conditions, with quicker responses possible when the driver is highly alert and the warning is clear. Therefore, for visualisation purposes, all TTC values exceeding 5 seconds are truncated to 5 seconds, as higher values are less relevant for practical decision-making.

Figure 8 shows the performance of the developed measures. Figure 8a, 8b illustrate the time to collision in the longitudinal and lateral directions between the car and the tractor, as well as the car and the semitrailer. Both versions predict a sideswipe collision (black solid line) between the car and the semitrailer. In versions 2 and 3, the initial prediction indicates a rear-end collision (green solid line) between the car and the semitrailer, which subsequently transitions into a sideswipe collision. This happens due to the car's rapid acceleration. Additionally, the noise in the signals observed in version 3 can be attributed to numerical errors introduced by the numerical integration process.

Figure 8c compares the  $TTC_{2D}$  formulations developed in this paper with the conventional TTC and the  $TTC_{2D}$  proposed by Guo et al. (2023). It is important to note that Guo et al. (2023) does not provide a methodology for applying their measure to articulated vehicles. Therefore, for the purpose of this comparison, their  $TTC_{2D}$  has been implemented using the methodology proposed in this paper. The same approach is also used to adapt the conventional TTC, which is inherently limited to predicting rear-end collisions. As a result, its behaviour closely resembles the rear-end collision patterns observed in Figures 8a and 8b.

Initially, the conventional TTC predicts a collision, but after approximately 16.4 seconds, it indicates no collision, suggesting different crossing times for the vehicles at the same location. While this reflects the absence of a rear-end

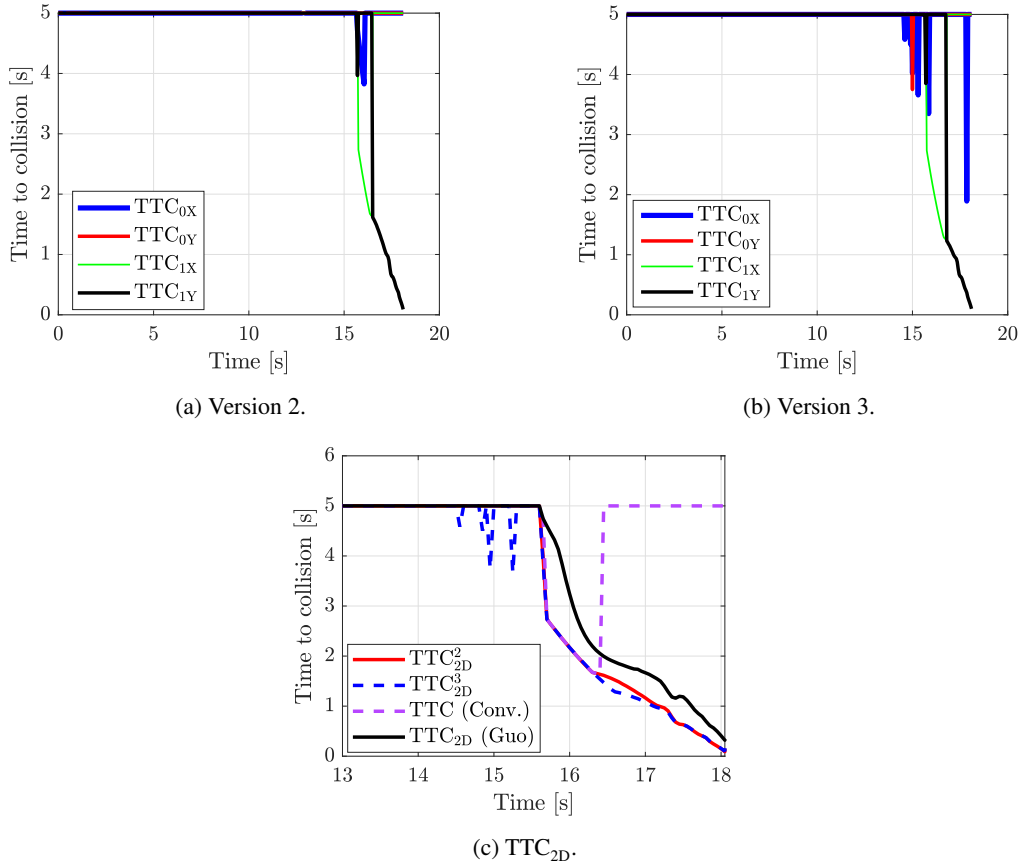


**Figure 8:** Comparison of TTC in the longitudinal and lateral directions between the car and the tractor, as well as the car and the semitrailer, for (a) version 2, and (b) version 3. (d) Evaluation of the developed  $TTC_{2D}$  versions against conventional TTC and  $TTC_{2D}$  from Guo et al. (2023).

collision, it fails to detect the actual sideswipe collision, which is correctly captured by the various  $TTC_{2D}$  versions. Versions 2 and 3 produce nearly identical results and clearly outperform both the conventional TTC and the original  $TTC_{2D}$  from Guo et al. (2023). For example, at 16 seconds, both versions predict a 2-second time to collision, which aligns well with the actual collision occurring at 18 seconds, whereas the existing  $TTC_{2D}$  overestimates this interval at 3 seconds. The similarity between Versions 2 and 3 can be attributed to the flattening of the speed curves for both vehicles toward the end of the scenario, as shown in Figure 7a. This likely reduces the impact of the additional acceleration information incorporated in Version 3.

## 6. Conclusions and Future work

This paper extends the existing measure  $TTC_{2D}$  by incorporating vehicle orientation and demonstrates its applicability to articulated vehicles such as a tractor-semitrailer. The objective of the measure is to predict rear-end and sideswipe collisions. The measure is developed through a sequential approach. The first version accounts for vehicle orientation while assuming constant heading and speed, without enforcing articulation constraints. The second version introduces articulation constraints while assuming constant speed and heading. Finally, the third version incorporates both articulation constraints and constant acceleration, while assuming a constant heading. The performance of these versions is then evaluated using a scenario created in CARLA.

All developed versions can predict rear-end collisions similar to conventional TTC while also capturing sideswipe collisions, which the latter cannot. Versions incorporating articulation constraints have similar performance and outperform the existing model in the literature. However, the inclusion of acceleration does not significantly enhance

performance and introduces noise due to numerical errors. Considering these factors, the version with articulation constraints and constant speed and heading seems to be more suitable for different ADAS applications.

Future research can further extend this  $TTC_{2D}$  to relax the constant heading assumption. In that case, the solution of (27) must be obtained through numerical integration instead of analytically solving it. Subsequently, for example, a constant curvature model can be used for the heading of the tractor. Sideswipe collisions are common for articulated vehicles at intersections. A similar scenario can be analysed to assess the performance of the proposed measure. Another research direction includes using the measure in the closed-loop simulation. For example, one can use it as a constraint to the MPC controller for a motion planning problem where TTC is mostly used. It is also interesting to explore the possibility of applying the measure to real-world vehicles. The measure can be computed using data from existing onboard sensors and cameras, such as LiDAR, radar, and vision systems.

## CRediT authorship contribution statement

**Abhijeet Behera:** Conceptualization, Methodology, Formal analysis, Investigation, Writing-original draft. **Sogol Kharrazi:** Conceptualization, Writing - review & editing, Supervision. **Erik Frisk:** Resources, Writing - review & editing, Supervision. **Maytheewat Aramrattana:** Funding acquisition, Writing - review & editing.

## Acknowledgements

This work has been funded by the European Union, under grant number 101069576.

## Data availability

Not applicable.

## Declaration of competing interest

The authors declare that they have no known competing financial interests or personal relationships that could have appeared to influence the work reported in this paper.

## Appendix A: Yaw angle computation

A vehicle is a system with non-holonomic constraints (Minaker and Rieveley, 2010). It can move forward and backward, however, can not move sideways without turning. Hence, the position and velocity of the vehicle can not be expressed purely as a function of the generalised coordinates describing the vehicle and often include higher derivatives. The non-holonomic constraint typically takes the form of a non-integrable differential equation given by,

$$f(q_1, q_2, \dots, q_n, \dot{q}_1, \dot{q}_2, \dots, \dot{q}_n) = 0, \quad (19)$$

where  $q_i$  are the generalised coordinates and  $\dot{q}_i$  their derivatives. Let  $\psi$  be the vehicle's orientation, and  $X$  and  $Y$  are the position coordinates of the axle in the global frame of reference. The non-holonomic constraint corresponding to one of the axles of the vehicle can be written as,

$$\dot{X} \sin \psi - \dot{Y} \cos \psi = 0. \quad (20)$$

Similar expressions can be obtained for a tractor-semitrailer combination. Figure 9 depicts the schematic of the tractor-semitrailer combination. The positions of the centre of axles in the global frame of reference ( $G$ ) are given as,

- Front axle of tractor:  $(X_{a0}, Y_{a0})$ ,
- Rear axle of tractor:  $(X_{b0}, Y_{b0})$ ,
- Rear axle of semitrailer:  $(X_{b1}, Y_{b1})$ ,

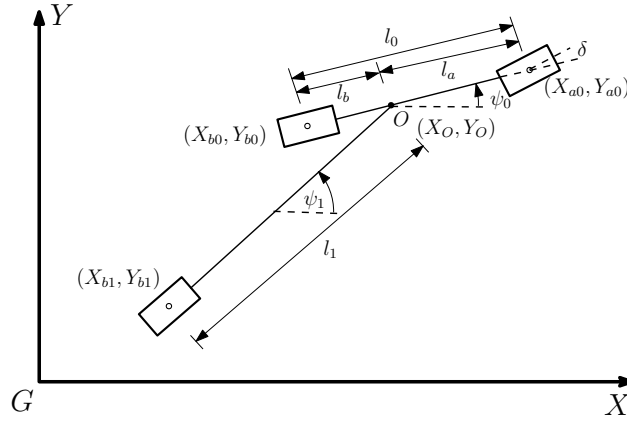


**Figure 9:** Schematic of tractor-semitrailer combination.

where the second subscript in the position, ‘0’ and ‘1’, denote the first (tractor) and second (semitrailer) units respectively. The articulation joint, denoted by ‘O’, is located at a distance of  $l_a$  and  $l_b$  from the tractor’s front and rear axle respectively. The rear axle of the semitrailer is located at  $l_1$  from the articulation joint. The yaw angle of the tractor is represented by  $\psi_0$ , whereas  $\psi_1$  indicates the yaw angle of the semitrailer. Furthermore,  $\delta$  denotes the steering angle of the first axle of the tractor. The non-holonomic constraints for the tractor-semitrailer combination depicted in Figure 9 are given by,

$$\dot{X}_{a0} \sin(\psi_0 + \delta) - \dot{Y}_{a0} \cos(\psi_0 + \delta) = 0, \quad (21a)$$

$$\dot{X}_{b0} \sin \psi_0 - \dot{Y}_{b0} \cos \psi_0 = 0, \quad (21b)$$

$$\dot{X}_{b1} \sin \psi_1 - \dot{Y}_{b1} \cos \psi_1 = 0. \quad (21c)$$

The following relations hold based on the kinematics of the combination.

$$X_{a0} = X_{b0} + l_0 \cos \psi_0, \quad (22a)$$

$$Y_{a0} = Y_{b0} + l_0 \sin \psi_0, \quad (22b)$$

$$X_{b1} = X_{b0} + l_b \cos \psi_0 - l_1 \cos \psi_1, \quad (22c)$$

$$Y_{b1} = Y_{b0} + l_b \sin \psi_0 - l_1 \sin \psi_1. \quad (22d)$$

Let  $u_{b0}$  represent the longitudinal velocity of the tractor’s rear axle. Assuming a small side-slip angle at the rear axle, the lateral velocity component  $v_{b0}$  is considered negligible. Under this assumption, the dynamics associated with the rear axle of the tractor can be expressed as follows,

$$\dot{X}_{b0} = u_{b0} \cos \psi_0 - v_{b0} \sin \psi_0 \approx u_{b0} \cos \psi_0, \quad (23a)$$

$$\dot{Y}_{b0} = u_{b0} \sin \psi_0 + v_{b0} \cos \psi_0 \approx u_{b0} \sin \psi_0. \quad (23b)$$

Differentiating the positions obtained in (22) followed by substitution of (23) results in,

$$\dot{X}_{a0} = u_{b0} \cos \psi_0 - l_0 \dot{\psi}_0 \sin \psi_0, \quad (24a)$$

$$\dot{Y}_{a0} = u_{b0} \sin \psi_0 + l_0 \dot{\psi}_0 \cos \psi_0, \quad (24b)$$

$$\dot{X}_{b1} = u_{b0} \cos \psi_0 - l_b \sin \psi_0 \dot{\psi}_0 + l_1 \dot{\psi}_1 \sin \psi_1, \quad (24c)$$

$$\dot{Y}_{b1} = u_{b0} \sin \psi_0 + l_b \cos \psi_0 \dot{\psi}_0 - l_1 \dot{\psi}_1 \cos \psi_1, \quad (24d)$$

Now, the yaw rate of the tractor ( $\dot{\psi}_0$ ) can be computed by substituting the expressions obtained from (24) in (21a).

$$\begin{aligned}
& \dot{X}_{a0} \sin(\psi_0 + \delta) - \dot{Y}_{a0} \cos(\psi_0 + \delta) = 0, \\
\Leftrightarrow & (u_{b0} \cos \psi_0 - l_0 \dot{\psi}_0 \sin \psi_0) \sin(\psi_0 + \delta) \cdots \\
& \quad - (u_{b0} \sin \psi_0 + l_0 \dot{\psi}_0 \cos \psi_0) \cos(\psi_0 + \delta) = 0, \\
\Leftrightarrow & (\cos \psi_0 \sin(\psi_0 + \delta) - \sin \psi_0 \cos(\psi_0 + \delta)) u_{b0} \cdots \\
& \quad - (\sin \psi_0 \sin(\psi_0 + \delta) + \cos \psi_0 \cos(\psi_0 + \delta)) \dot{\psi}_0 l_0 = 0, \\
\Leftrightarrow & u_{b0} \sin \delta - l_0 \dot{\psi}_0 \cos \delta = 0, \\
\Leftrightarrow & \dot{\psi}_0 = \frac{u_{b0} \tan \delta}{l_0}.
\end{aligned} \tag{25}$$

The yaw rate of the semitrailer ( $\dot{\psi}_1$ ) can be computed by substituting the expressions obtained from (24) in (21c).

$$\begin{aligned}
& \dot{X}_{b1} \sin \psi_1 - \dot{Y}_{b1} \cos \psi_1 = 0, \\
\Leftrightarrow & (u_{b0} \cos \psi_0 - l_b \sin \psi_0 \dot{\psi}_0 + l_1 \dot{\psi}_1 \sin \psi_1) \sin \psi_1 \cdots \\
& \quad - (u_{b0} \sin \psi_0 + l_b \cos \psi_0 \dot{\psi}_0 - l_1 \dot{\psi}_1 \cos \psi_1) \cos \psi_1 = 0, \\
\Leftrightarrow & u_{b0} \sin(\psi_1 - \psi_0) - l_b \dot{\psi}_0 \cos(\psi_1 - \psi_0) + l_1 \dot{\psi}_1 = 0, \\
\Leftrightarrow & \dot{\psi}_1 = \frac{l_b \dot{\psi}_0 \cos(\psi_1 - \psi_0) - u_{b0} \sin(\psi_1 - \psi_0)}{l_1}, \\
\Leftrightarrow & \dot{\psi}_1 = \frac{u_{b0} \tan \delta}{l_0} \frac{l_b}{l_1} \cos(\psi_1 - \psi_0) - \frac{u_{b0}}{l_1} \sin(\psi_1 - \psi_0).
\end{aligned} \tag{26}$$

In the case where the tractor is driving straight, the heading of the tractor is constant, i.e  $\dot{\psi}_0 = 0$ . For this case, (26) can further be simplified to,

$$\dot{\psi}_1 = -\frac{u_{b0}}{l_1} \sin(\psi_1 - \psi_0(t_0)), \tag{27}$$

where  $\psi_0(t_0)$  denotes the initial yaw angle of the tractor. An analytical expression for the yaw angle of the semitrailer can be computed by integrating the yaw rate obtained in (27). The expression for the yaw angle of the semitrailer is given by,

$$\begin{aligned}
& \int_{\psi_1(t_0)}^{\psi_1(t)} \frac{1}{\sin(\psi_1 - \psi_0(t_0))} d\psi_1 = \int_{t_0}^t -\frac{u_{b0}}{l_1} dt, \\
& \ln \frac{|\csc(\psi_1(t) - \psi_0(t_0)) - \cot(\psi_1(t) - \psi_0(t_0))|}{|\csc(\psi_1(t_0) - \psi_0(t_0)) - \cot(\psi_1(t_0) - \psi_0(t_0))|} = \frac{u_{b0}}{l_1} (t_0 - t), \\
& |\csc(\psi_1(t) - \psi_0(t_0)) - \cot(\psi_1(t) - \psi_0(t_0))| = \cdots \\
& \quad |\csc(\psi_1(t_0) - \psi_0(t_0)) - \cot(\psi_1(t_0) - \psi_0(t_0))| \exp\left(\frac{u_{b0}}{l_1} (t_0 - t)\right), \\
& \left| \tan \frac{\psi_1(t) - \psi_0(t_0)}{2} \right| = \left| \tan \frac{\psi_1(t_0) - \psi_0(t_0)}{2} \right| \exp\left(\frac{u_{b0}}{l_1} (t_0 - t)\right), \\
& \psi_1(t) = \begin{cases} \psi_0(t_0) + 2 \arctan\left(\left| \tan \frac{\psi_1(t_0) - \psi_0(t_0)}{2} \right| \exp\left(\frac{u_{b0}}{l_1} (t_0 - t)\right)\right) : (\psi_1(t-1) - \psi_0(t_0) < 0), \\ \psi_0(t_0) - 2 \arctan\left(\left| \tan \frac{\psi_1(t_0) - \psi_0(t_0)}{2} \right| \exp\left(\frac{u_{b0}}{l_1} (t_0 - t)\right)\right) : (\psi_1(t-1) - \psi_0(t_0) > 0). \end{cases}
\end{aligned} \tag{28}$$

The above integration is performed by assuming a constant speed ( $u_{b0}$ ). When the speed is not constant,  $u_{b0}$  is reformulated using (23a) and is given by,

$$u_{b0} = \frac{\dot{X}_{b0}}{\cos \psi_0}. \tag{29}$$

Substituting the expression for  $u_{b0}$  into (27), and performing the subsequent integration, the yaw angle of the semitrailer for non-constant speed is obtained as,

$$\begin{aligned}
& \int_{\psi_1(t_0)}^{\psi_1(t)} \frac{1}{\sin(\psi_1 - \psi_0(t_0))} d\psi_1 = \int_{t_0}^t -\frac{u_{b0}}{l_1} dt, \\
& \ln \frac{|\csc(\psi_1(t) - \psi_0(t_0)) - \cot(\psi_1(t) - \psi_0(t_0))|}{|\csc(\psi_1(t_0) - \psi_0(t_0)) - \cot(\psi_1(t_0) - \psi_0(t_0))|} = \int_{t_0}^t -\frac{\dot{X}_{b0}}{l_1 \cos \psi_0} dt, \\
& \left| \tan \frac{\psi_1(t) - \psi_0(t_0)}{2} \right| = \left| \tan \frac{\psi_1(t_0) - \psi_0(t_0)}{2} \right| \exp\left(\frac{X_{b0}(t_0) - X_{b0}(t)}{l_1 \cos \psi_0}\right), \\
& \psi_1(t) = \begin{cases} \psi_0(t_0) + 2 \arctan\left(\left| \tan \frac{\psi_1(t_0) - \psi_0(t_0)}{2} \right| \exp\left(\frac{X_{b0}(t_0) - X_{b0}(t)}{l_1 \cos \psi_0}\right)\right) : (\psi_1(t-1) - \psi_0(t_0) < 0), \\ \psi_0(t_0) - 2 \arctan\left(\left| \tan \frac{\psi_1(t_0) - \psi_0(t_0)}{2} \right| \exp\left(\frac{X_{b0}(t_0) - X_{b0}(t)}{l_1 \cos \psi_0}\right)\right) : (\psi_1(t-1) - \psi_0(t_0) > 0). \end{cases}
\end{aligned} \tag{30}$$

## References

- Abdel-Aty, M., Pande, A., 2007. Crash data analysis: Collective vs. individual crash level approach. *Journal of Safety Research* 38, 581–587.
- Attard, D., Bajada, J., 2024. Autonomous navigation of tractor-trailer vehicles through roundabout intersections. *arXiv preprint arXiv:2401.04980*.
- Behera, A., Kharrazi, S., Frisk, E., 2025. Collision avoidance analysis of an articulated heavy vehicle in carla, in: *The IAVSD International Symposium on Dynamics of Vehicles on Roads and Tracks*.
- Dosovitskiy, A., Ros, G., Codevilla, F., Lopez, A., Koltun, V., 2017. Carla: An open urban driving simulator, in: *Conference on robot learning*, PMLR. pp. 1–16.
- Guo, H., Xie, K., Keyvan-Ekbatani, M., 2023. Modeling driver's evasive behavior during safety-critical lane changes: Two-dimensional time-to-collision and deep reinforcement learning. *Accident Analysis & Prevention* 186, 107063.
- Haué, J.B., Merlhiot, G., 2024. How do automated vehicles influence other road users and sometimes elicit uncivil behaviors?, in: *Proceedings of the 16th International Conference on Automotive User Interfaces and Interactive Vehicular Applications*, pp. 374–383.
- Hayward, J., 1971. Near misses as a measure of safety at urban intersections. *Pennsylvania Transportation and Traffic Safety Center*.
- Hayward, J.C., 1972. Near miss determination through use of a scale of danger.
- He, Z., Qin, X., Liu, P., Sayed, M.A., 2018. Assessing surrogate safety measures using a safety pilot model deployment dataset. *Transportation research record* 2672, 1–11.
- Hou, J., List, G.F., Guo, X., 2014. New algorithms for computing the time-to-collision in freeway traffic simulation models. *Computational intelligence and neuroscience* 2014, 761047.
- Johnsson, C., Laureshyn, A., De Ceunynck, T., 2018. In search of surrogate safety indicators for vulnerable road users: a review of surrogate safety indicators. *Transport reviews* 38, 765–785.
- Mahmud, S.S., Ferreira, L., Hoque, M.S., Tavassoli, A., 2017. Application of proximal surrogate indicators for safety evaluation: A review of recent developments and research needs. *IATSS research* 41, 153–163.
- Minaker, B., Rieveley, R., 2010. Automatic generation of the non-holonomic equations of motion for vehicle stability analysis. *Vehicle system dynamics* 48, 1043–1063.
- Minderhoud, M.M., Bovy, P.H., 2001. Extended time-to-collision measures for road traffic safety assessment. *Accident Analysis & Prevention* 33, 89–97.
- Morando, M.M., Tian, Q., Truong, L.T., Vu, H.L., 2018. Studying the safety impact of autonomous vehicles using simulation-based surrogate safety measures. *Journal of advanced transportation* 2018, 6135183.
- Nikolaou, D., Ziakopoulos, A., Yannis, G., 2023. A review of surrogate safety measures uses in historical crash investigations. *Sustainability* 15, 7580.
- Ozbay, K., Yang, H., Bartin, B., Mudigonda, S., 2008. Derivation and validation of new simulation-based surrogate safety measure. *Transportation research record* 2083, 105–113.
- Sarkar, D.R., Rao, K.R., Chatterjee, N., 2024. A review of surrogate safety measures on road safety at unsignalized intersections in developing countries. *Accident Analysis & Prevention* 195, 107380.
- So, J.J., Dedes, G., Park, B.B., HosseinyAlamdary, S., Grejner-Brzezinski, D., 2015. Development and evaluation of an enhanced surrogate safety assessment framework. *Transportation research part C: emerging technologies* 50, 51–67.
- Tarko, A.P., 2018. Surrogate measures of safety, in: *Safe mobility: challenges, methodology and solutions*. Emerald Publishing Limited. volume 11, pp. 383–405.
- Tidwell, S., Blanco, M., Trimble, T., Atwood, J., Morgan, J., 2015. Evaluation of heavy-vehicle crash warning interfaces (no. dot hs 812 191). *National Highway Traffic Safety Administration*.
- Wang, C., Xie, Y., Huang, H., Liu, P., 2021. A review of surrogate safety measures and their applications in connected and automated vehicles safety modeling. *Accident Analysis & Prevention* 157, 106157.

- Ward, J.R., Agamennoni, G., Worrall, S., Bender, A., Nebot, E., 2015. Extending time to collision for probabilistic reasoning in general traffic scenarios. *Transportation Research Part C: Emerging Technologies* 51, 66–82.
- Xie, K., Yang, D., Ozbay, K., Yang, H., 2019. Use of real-world connected vehicle data in identifying high-risk locations based on a new surrogate safety measure. *Accident Analysis & Prevention* 125, 311–319.